*Title Page

Lower grade gliomas: relationships between metabolic and structural imaging with grading and molecular factors

Marco Riva[1,2]* M.D., Egesta Lopci[3]* M.D. Ph.D., Antonella Castellano[4] M.D. Ph.D., Laura Olivari[3] M.D, Marcello Gallucci[5] Ph.D., Federico Pessina[2] M.D., Bethania Fernandes[6] M.D., Matteo Simonelli[7-8] M.D., Pierina Navarria[9] M.D., Marco Grimaldi[10] M.D., Roberta Rudà[11] M.D., Angelo Castello[3] M.D., Marco Rossi[2] M.D., Tommaso Alfiero[2] M.D., Riccardo Soffietti[11] M.D., Arturo Chiti[3,12] M.D. and Lorenzo Bello[2,13] M.D.

1. Department of Medical Biotechnology and Translational Medicine, Università degli Studi di Milano, Milan (MI), ITALY
2. Unit of Oncological Neurosurgery, Humanitas Research Hospital, Rozzano (MI), ITALY
3. Unit of Nuclear Medicine, Humanitas Research Hospital, Rozzano (MI), ITALY
4. Neuroradiology Unit and CERMAC, Vita-Salute San Raffaele University and IRCCS San Raffaele Scientific Institute, Milan (MI), ITALY
5. Faculty of Psychology, Università di Milano Bicocca, Milan (MI), ITALY
6. Pathology Unit, Humanitas Research Hospital, Rozzano (MI), ITALY
7. Department of Biomedical Sciences, Humanitas University, Rozzano (MI), ITALY
8. Humanitas Cancer Center, Humanitas Research Hospital, Rozzano (MI), IT AL Y
9. Radiotherapy and Radiosurgery Unit, Humanitas Research Hospital, Rozzano (MI), ITALY
10. Neuroradiology Unit, Humanitas Research Hospital, Rozzano (MI), ITALY
11. Department of Neuro-Oncology, University and City of Health and Science Hospital, Turin, (TO), ITALY.

12. Humanitas University, Rozzano (MI), ITALY
13. Department of Oncology and Hemato-oncology, Università degli Studi di Milano, Milan (MI), ITALY

*These authors contributed equally to this work.

Corresponding Author

Marco Riva, M.D.

Department of Medical Biotechnology and Translational Medicine, Università degli Studi di Milano, Via Manzoni 56, 20089 – Rozzan (MI), ITALY

E-mail: marco.riva@unimi.it

Keywords: Clinical trials Observational study, MRI, PET, Primary brain tumor, Surgical therapy - tumor

Running head: 11C-MET-PET metrics and histomolecular features in LGGs

Disclosure of funding: M.Ri. was supported by the Fellowship for Abroad 2013 of the Fondazione Italiana per la Ricerca sul Cancro (FIRC)

No potential conflicts of interest relevant to this article exist

Word Count

Manuscript: 4998 words

***Disclosure-Conflict of Interest [authors to provide own statement, .doc(x) format preferred]**

Click here to download Disclosure-Conflict of Interest [authors to provide own statement, .doc(x) format preferred]: 00_COI.docx

ABBREVIATIONS LIST

11C-METH-PET: carbon-11-methionine PET

1p19q codeletion: codeletion of chromosome arms 1p and 19q

EANO: European Association of Neuro-oncology

IDH: isocitrate dehydrogenase

LGGs: lower grade gliomas

MTB: metabolic tumor burden

PET: positron emission tomography

RANO: Response Assessment in Neuro-Oncology

ROI: region of interest

SUV: Standard Uptake Value

WHO: World Health Organization

ABSTRACT

Background: positron emission tomography (PET) is a valuable tool for the characterization of brain tumors *in vivo*; yet, few studies investigated the correlations between 11C-METH PET metrics and the clinico-radiological, histological and molecular features in patients affected by lower grade gliomas (LGGs). This observational study aimed at evaluating the relationships between carbon-11-methionine PET (11C-METH PET) metrics and structural MRI imaging with histo-molecular biomarkers in patients with LGGs candidate to surgery.

Methods: 96 patients with pathologically proven LGGs (51 males, 45 females; age 44.1±13.7 years; 45 grade II, 51 grade III), referred from March 2012 to January 2015 for tumor resection and submitted to pre-operative 11C-METH PET were enrolled. Semi-quantitative metrics for 11C-METH PET included Standard Uptake Value (SUV) max, SUV ratio to normal brain and metabolic tumor burden (MTB). PET semiquantitative metrics were analyzed and compared to MRI features, histological diagnosis, IDH-1/2 status and 1p/19q co-deletion.

Results: Histological grade was associated with SUV Max (p=0.002), SUV ratio (p=0.011) and MTB (p.=0.001), with grade III lesions showing higher metrics. Among nonenhancing lesions on MRI, SUVmax (p=0.001), SUVratio (p=0.003) and MTB (p<0.001) were statistically different in grade II versus grade III. MRI lesion volume poorly correlated with MTB (r^2=0.13). SUVmax and the SUVratio were higher (p<0.05) in IDH-1/2 wild-type lesions, while SUVratio was associated with the presence of 1p19q codeletion.

Conclusions: 11C-METH PET metrics significantly correlate with histological grade and molecular profile. PET semiquantitative metrics can improve pre-surgical evaluation of LGGs and thus support the clinical decision-making.

INTRODUCTION

World Health Organization (WHO) Grade II and III gliomas are tumors of the central nervous system (CNS) defined as lower-grade gliomas (LGGs) upon the clinical behavior and molecular stratification[1–3].

The updated WHO classification[1] considers both histologic and molecular parameters as crucial for an integrated diagnosis. However, the coexistence of areas with different histological and biological characteristics in the same tumor can impair the possibility to reach a correct diagnosis.

Conventional MRI is the standard modality for the pre-operative characterization of a primary brain tumor[4,5], but LGGs often show absence of contrast enhancement in the early stages of progression, which can lead to an underestimation of tumor grading[4,6].

Positron emission tomography (PET) with radiolabelled amino-acids, like L-methyl-C11-methionine (11C-METH), has been proven to be a valuable tool for the in vivo characterization of brain tumors. It has been shown that 11C-METH PET can differentiate gliomas[7–11], it can provide prognostic information prior to surgery[12–16], it can be used for radiation therapy planning[17,18], and it has a high diagnostic accuracy in the detection of glioma recurrence[19]. Based upon these evidences, several international working groups, such as the Response Assessment in Neuro-Oncology (RANO) and the European Association of Neuro-oncology (EANO), recommended the additional use of amino acid PET imaging at every stage of brain tumor management[20,21].

Nevertheless, few studies evaluated the correlations between 11C-METH PET semi-quantitative and qualitative metrics and the clinico-radiological, histological and molecular features in LGGs. The aim of this observational study was thus to characterize the relationships between 11C-METH PET metrics, conventional MRI parameters, histological and molecular factors and clinical features of patients undergoing surgical resection.

METHODS

Patients' population

A series of 96 patients (51 males, 45 females; age 44.1±13.7 years) affected by LGGs (i.e. grade II and III), who underwent a craniotomy for tumor resection from March 2012 to January 2015, was analyzed in this observational cohort study (NCT02518061). All patients had 11C-METH PET performed within 30 days before surgery, adequate tumor specimen following surgery and fully available clinical data including complete follow-up. Demographic profile and clinical-radiological features are reported in [**Table 1**]. Pathological diagnosis was performed according to according to the 2007 WHO Brain Tumor Classification[22]. This study was conducted with the approval (#1481) of the local ethic committee.

11C-METH PET imaging

Before surgery, all patients performed 11C-METH PET. The radiopharmaceutical, carrier-free L-(methyl-11C)-methionine, was synthesized on-site using a General Electric TracerLab FXc synthesis module with the method previously described[12]. A total amount of 300-500MBq, was administered in patients who had been fasting for at least 4 hours. Images were acquired 15 minutes later on a PET/CT tomograph, either a Biograph 6 LSO scanner (Siemens Medical Systems, Erlangen, Germany) or a Discovery 690 GE scanner (General Electric Healthcare, Waukesha, WI). CT attenuation-corrected 3D images were acquired for 10min from the scalp to vertebra C3 level and images were subsequently reconstructed using an iterative reconstruction algorithm (OSEM) and displayed on GE Adw4.6 Workstation. Images were reconstructed and acquired in order to minimize differences in semi-quantitative evaluations related to the use of two different scanners.

Data obtained by 11C-METH PET were analyzed by board-certified Nuclear Medicine physicians, and then revised based on a semi-quantitative scale. SUVmax (maximum

standardized uptake value), SUVratio and metabolic tumor burden (MTB) were considered as semi-quantitative parameters. SUVratio was obtained as the ratio between count rates determined in the region of interest (ROI) drawn in the tumor area with the highest uptake of 11C-METH (SUVmax) and the count rates in a corresponding ROI drawn in the contralateral side. The values were corrected for injected activity and adjusted to the patient's weight. Tumor volumes as found on PET were then delineated automatically with a dedicated workstation software package, the GE PETVCAR® (PET Volume Computer Assisted Reading), based on an estimated threshold weight of 50%. When needed, the volume was adjusted manually by visual thresholding. MTB was computed as the volume (expressed in cm^3) delineated on 11C-METH PET by the ROI of the entire tumor extent.

MRI Evaluation

Volumetric MRI sequences were acquired preoperatively on all patients with a 3 Tesla MR scanner (Siemens Verio, Erlangen, Germany) on the day before surgery. Image evaluation was performed by a board-certified neuroradiologist, blinded to nuclear medicine data. Volumes were computed with iPlan Cranial 3.0 software suite (Brainlab, Munich, Germany) from T2-weighted hyperintense lesions on Fluid-attenuated-inversion-recovery (FLAIR) and from gadolinium enhancing T1-weighted lesions by manual delineation of the lesion borders on all involved slices. The pre-operative MRI dataset was coregistered with a CT head scan with 7 radiolucent fiducials and the 11-C-METH-PET with iPlan Cranial 3.0 software. The coregistered dataset was then available for image guidance during surgery on a neuronavigation platform (Brainlab Curve, Brainlab AG, Munich, Germany).

Surgical Protocol

All patients gave written informed consent to the surgical procedure. Surgery was performed with the aid of a multimodal electrophysiological monitoring and intraoperative stimulation mapping for motor and language functions, under asleep or awake anesthesia according to the

surgical indications[23,24]. An ultrasound machine (Prosound Alpha7, Hitachi Aloka Medical Ltd, Zurich, Switzerland) with a pre-calibrated multi-frequency (3.75-10 MHz) convex transducer footprint 20 mm was employed[25]. A rigid array with 3 optic references was mounted onto the transducer to have it integrated with the neuronavigation in order to guide the tissue sampling in vivo and to acknowledge possible shifting of the regions of interest.

Pathological assessment

Tumor grading was performed on slides in hematoxylin and eosin (H&E) according to WHO International Histological Classification of Tumors[22]. IDH-1 mutational analysis was conducted with immunohistochemistry using antibody to IDH R132H and wildtype cases were then validated by PCR reaction. 1p/19q co-deletion status was assessed with fluorescence in situ hybridization (FISH, Vysis 1p36/1q25 e 19q13/19p13): deletions of 1p and 19q were defined as 33% of tumor nuclei containing the LOH pattern. **Table S1** reports the integrated diagnosis of the histopathological grading and the molecular profiles. The cell proliferation index was measured with immunohistochemistry using the MIB-1 antibody against Ki-67 protein.

Statistical analyses

An analysis of variance (ANOVA) was employed to explore the relationship among the PET metrics, as measured by semiquantitative parameters, and clinico-radiological features. Differences between rates were compared by the Chi square analysis. T-test was used to investigate differences between scanners (Siemens versus GE) for semiquantitative parameters.

To investigate the relationship among metabolic metrics and the 3 molecular subgroups, the PET metrics were analyzed with ANOVA on the natural log of the dependent variable (the F-test) and with a non-parametric Kruskal-Wallis test, due to distributional concerns.

For rank correlation, a Spearman' correlation coefficient (rho) and linear regression test were used. Sensitivity, specificity and accuracy in characterizing grade (i.e. grade II vs III) was computed to estimate the power of each parameter to discriminate between the two grade classes. A study of optimal cut-off and of the accuracy was then using Receiver Operating Characteristic (ROC) curve analysis. A multivariate analysis was performed to test the relationship among PET semi-quantitative parameters and other radiological and molecular features.

Statistical significance was set at $p \leq 0.05$ for each evaluation.

RESULTS

PET semi-quantitative metrics and histological grade

According to the WHO classification 2007, the distribution of brain tumors was as follows: 26 grade II and 15 grade III oligodendrogliomas, 8 grade II and 22 grade III astrocytomas, 11 grade II and 14 grade III oligoastrocytomas. Forty-eight tumors were newly diagnosed and treatments naive and 48 recurrent [**Table 1**].

The mean proliferative index, as measured by the MIB-1, was different between grades: i.e. 3.0 for grade II and 13.3 for grade III ($p<0.001$). The proliferative index was related to SUVmax ($F(1.92)=4.3$, $p=0.04$), SUVratio ($F(1.92)=4.2$, $p=0.04$) and MTB ($F(1.92)=9.8$, $p=0.002$).

Mean SUVmax was 3.5±1.7 (range 1.0-9.2), mean SUVratio 2.3±1.1 (range 1.1-8.3), mean MTB 33.13 (range 0.3-250.3). On T-test there was no difference between scanners for all semiquantitative parameters ($p>0.05$). When analyzed according to grade, a statistically significant difference was observed for SUVmax, SUVratio and MTB values between grade II and III. In particular, grade was related to SUVmax ($F(1,94)=18.56$, $p<0.001$), SUV ratio ($F(1,94)=13.46$, $p<0.01$ and MTB ($F(1,94)=21.58$, $p<0.0001$), with grade III lesions showing higher values for all metrics [**Figure S1A-C**].

PET semi-quantitative metrics and MRI findings

Sixty-nine patients had no enhancement, while 27 had a variable degree of enhancement on pre-operative MRI [**Table 1**]. Patients with contrast enhancement displayed statistically significant higher PET semiquantive values: SUVmax ($F(1.94)=15.4$, $p<0.001$), SUVratio ($F(1.94)=12.4$, $p=0.001$) and MTB ($F(1.94)=6.9$, $p=0.01$) were all related to the gadolinium enhancement.

Among nonenhancing LGGs [69 individuals, **Table 2**], SUVmax (p=0.001), SUVratio (p=0.003) and MTB (p<0.001) were all statistically different in grade II versus grade III lesions: SUVmax, SUVratio and MTB in nonenhancing grade-2 LGGs were on average, 2.4±1.2, 1.7±0.6 and 7.1±0.9, respectively, compared to 3.6±1.4, 2.2±0.6and 28.8±1.0 for nonenhancing grade-3 LGGs. [**Figure 1A-B**] reports representative examples.

The MRI lesion volume was correlated only to MTB (F(1.93)=9.9, p=0.002) but not SUVmax or SUVratio: however, the correlation between MRI volume and MTB was modest (r^2=0.13) [**Figure S2**].

Accuracy, sensitivity and specificity of lesion characterization by PET and MRI

Accuracy, sensitivity and specificity of the three PET measurements in discriminating between grade II and III was evaluated. Results showed an overall good accuracy, especially concerning specificity. Grade was statistically predicted by SUVmax (p<0.001), SUVratio (p=0.002) and also MTB (p<0.001). Optimal cut-off values were 2.7, 2.0 and 14.9 for SUVmax, SUVratio and MTB, respectively [**Table 3**].

To assess whether the combination of PET parameters and MRI features, namely the presence of contrast enhancement, is superior in the diagnostic accuracy to discriminate between grade II and III a further analysis was performed. In particular, the likelihood of a grade III lesion is higher when contrast enhancement co-exists with higher PET semiquantitative values; an overall gain in accuracy, sensitivity and specificity is observed, as reported in [**Table 4**] compared to MR or PET alone.

PET semi-quantitative metrics and molecular features

The relationships between metabolic parameters and molecular features was explored, constraining the analysis to newly diagnosed lesions.

Both SUVmax and the SUVratio were significantly higher ($p<0.05$) in IDH-1/2 wild-type lesions (no. 28) compared to mutated lesions (no. 20) [**Figure 2A**], while SUVratio was associated with the presence of 1p19q codeletion only, having 1p19q codeleted lesions a lower SUVratio [**Figure 2B**].

On multivariate analysis, SUVmax only was found significantly correlated with IDH status ($p = 0.02$), while other parameters, such as SUVratio, histological grade and presence of contrast enhancement, were not associated with the mutational status of IDH.

A trend toward a correlation between PET semiquantitative metrics and the 3 molecular subgroups of the new WHO classification of 2016, i.e. IDH-1/2 mutated and 1p19 codeleted lesions, IDH-1/2 mutated and 1p19q not codeleted lesions and IDH-1/2 wild-type lesions, was evident, but not statistically significant [**Figure 3**].

DISCUSSION

LGGs display a variable prognosis, that is predicted by molecular factors[3,21] in addition to clinical variables, such as age at diagnosis[26], tumor volume[27], speed of growth[28] and extent of surgical resection[27,29]. The updated WHO classification of the CNS tumors of 2016 now includes both conventional histological parameters and molecular factors in an integrated diagnosis[1]. In particular, isocitrate dehydrogenases (IDH) status and codeletion of chromosome arms 1p and 19q (1p/19q codeletion), have been shown to capture the biologic characteristics of LGGs with greater sensitivity compared to histological classification alone[30], which can be hampered by both interobserver variability and sampling error during surgery.

Positron emission tomography (PET) with radiolabelled amino-acids, like L-methyl-C11-methionine (11C-METH), has been proven to be a valuable tool for the in vivo characterization of primary brain tumors[31]. 11C-METH PET can discriminate high from low grade gliomas[7,9–12], provide prognostic information prior to surgery[13–16,32] and be used for radiation therapy planning[17,18]; it also has a high diagnostic accuracy in the detection of glioma recurrence[19].

Based on a previous investigation[12], the current study evaluated the additional benefit of metabolic imaging with 11C-METH-PET in the management of LGGs. Gliomas are heterogeneous tumors[33–35], in whom the identification of the extent of infiltration and aggressive tumor components is relevant in planning surgery and performing sampling of the most representative tissue for a correct diagnosis. In this regard, conventional MRI has a limited definition of the heterogeneity and extension of gliomas; therefore, it has been questioned whether structural imaging only is able to appropriately guide the resection and the sampling or whether metabolic imaging should also be included, especially in case of

non-enhancing lesions[36]. The RANO working group[20] and the EANO[21] both recommended the use of amino acid PET as an additional tool for evaluating gliomas.

To date, few studies investigated in LGGs the correlations of metabolic and structural MRI findings with molecular features and histological grade[37,38]. Among these studies, few only examined imaging findings in the context of the new WHO brain tumor classification[12,15,39]. Although the pathological diagnosis was still based on the 2007 WHO classification[22], given the retrospective design, and this representing a limitation of the current observational study, a robust relationship among glioma grade and 11C-METH-PET semiquantitative metrics was found in several aspects: imaging with 11C-METH-PET can help in the distinction among nonenhancing gliomas on MRI between grade II and grade III tumors and higher values of SUVmax, SUVratio and MTB were significantly associated with Grade 3 lesions compared to Grade 2 lesions.

No significant correlation was found between MRI volume and PET metrics [**Figure S2**]. This is not surprising because anaplastic areas, that can be detected by PET, co-exist with more differentiated areas without modifying the MRI volume in LGGs. The metabolic findings could thus be regarded as an additional non-invasive *in vivo* pre-operative biomarker of LGGs aggressiveness, along with an increase of lesion volume[27] and speed of growth[28].

The combination of 11C-METH PET and conventional MRI enabled a more refined preoperative diagnosis. Diagnostic accuracy, sensitivity and, to a lower extent, specificity were improved when 11C-METH PET and conventional MRI were combined, reaching values of accuracy and specificity as high as 75% and 87%, respectively. The combination of the diagnostic yield of MRI with that of PET, in particular of the SUVmax, could be regarded as a promising approach for a better pre-treatment work-up of presumed LGGs [**Figure 4**], especially with an increasing use of hybrid MRI-PET facilities world-wide[40].

In this study, we also found a significant association between IDH status and PET parameters, as IDH-1/2 wild-type lesions displayed a higher metabolic activity than IDH-1/2 mutated LGGs in terms of SUVmax and SUVratio, while 1p19q codeleted lesions had a lower SUVratio. The latter finding, i.e. the relationship between the 1p19q loss of heterozygosity (LOH) and PET metrics can appear controversial when compared to earlier studies[15], where LGGs with 1p19q codeletion displayed higher uptake of PET tracers. However, a more recent study found that 11C-METH-PET metrics were significantly higher in oligodendroglial lesions without 1p/19q deletion especially when the tumor to normal brain ratio was analyzed[39], as in this study. This discrepancy could be explained by several factors, such as heterogeneity of different clinical cohorts and different percentages of true astrocytic and oligodendroglial lesions[41]. In addition, it could be argued that tumors without 1p/19q deletion are less likely to have IDH1 mutation and this can lead to a more active metabolism than those with the deletions[2,41].

When we analyzed the 3 molecular subgroups we restricted the analysis to newly diagnosed lesions. IDH-1/2 wild-type lesions displayed a higher metabolic activity than IDH-mutated/1p19 codeleted lesions and IDH-mutated/1p19q-not-codeleted lesions, as measured with SUVmax and SUVratio; however, the difference did not reach statistically significance. This could be due to either the small number of patients in each subgroup or the high relative fraction of IDH-wild type lesions. Further studies are thus needed to prove whether this interesting preliminary finding can be confirmed with a greater sample size and, hopefully a prospective design[42]. where the new WHO brain tumor classification can be considered *ab initio*.

Some attention must be paid to acquisition protocols and reconstruction algorithms, particularly in the context of multiple scanner types or in multicentric settings, since the inter and intra-center comparability of PET data should be based on harmonized criteria. In

addition, when a robust correlation between imaging data and other patient's pathological features is demonstrated, quantitative diagnostic findings could guide the choice of the site of tissue sampling, as it was done in the current study, where samples from hypermetabolic areas were sent separately for the histopathological diagnosis. This approach can reduce the errors in the histopathological evaluation, that are due to both sampling errors and interobserver variability[43].

CONCLUSION

Although retrospective, this observational study provided further evidence of the diagnostic power of 11C-MET PET in providing a refined pre-surgical evaluation of patients affected by presumed LGGs.

The information gained on the metabolism of the lesions are of potential clinical impact for guiding treatment decisions[44] in a patient-specific approach[45], adding relevant clues about the site of tissue sampling for a proper integrated histomolecular diagnosis.

PET imaging and the derived semiquantitative metrics can thus be considered relevant, along with other imaging techniques such as advanced MRI, to improve the non-invasive *in-vivo* characterization of LGGs and, ultimately, to promote an improved care and outcome of patients.

REFERENCES

1. Louis DN, Perry A, Reifenberger G, et al. The 2016 World Health Organization Classification of Tumors of the Central Nervous System: a summary. *Acta Neuropathol*. 2016;131(6):803-820. doi:10.1007/s00401-016-1545-1
2. Cancer Genome Atlas Research Network, Brat DJ, Verhaak RGW, et al. Comprehensive, Integrative Genomic Analysis of Diffuse Lower-Grade Gliomas. *N Engl J Med*. 2015;372(26):2481-2498. doi:10.1056/NEJMoa1402121
3. Aoki K, Nakamura H, Suzuki H, et al. Prognostic relevance of genetic alterations in diffuse lower-grade gliomas. *Neuro Oncol*. 2018;20(1):66-77. doi:10.1093/neuonc/nox132
4. Law M, Yang S, Wang H, et al. Glioma grading: sensitivity, specificity, and predictive values of perfusion MR imaging and proton MR spectroscopic imaging compared with conventional MR imaging. *AJNR Am J Neuroradiol*. 24(10):1989-1998. http://www.ncbi.nlm.nih.gov/pubmed/14625221. Accessed June 11, 2018.
5. Castellano A, Falini A. Progress in neuro-imaging of brain tumors. *Curr Opin Oncol*. 2016;28(6):484-493. doi:10.1097/CCO.0000000000000328
6. Plotkin M, Blechschmidt C, Auf G, et al. Comparison of F-18 FET-PET with F-18 FDG-PET for biopsy planning of non-contrast-enhancing gliomas. *Eur Radiol*. 2010;20(10):2496-2502. doi:10.1007/s00330-010-1819-2
7. Herholz K, Hölzer T, Bauer B, et al. 11C-methionine PET for differential diagnosis of low-grade gliomas. *Neurology*. 1998;50(5):1316-1322. http://www.ncbi.nlm.nih.gov/pubmed/9595980. Accessed June 11, 2018.
8. Lopci E, Riva M, Olivari L, et al. Prognostic value of molecular and imaging biomarkers in patients with supratentorial glioma. *Eur J Nucl Med Mol Imaging*. 2017;44(7):1155-1164. doi:10.1007/s00259-017-3618-3

9. Shinozaki N, Uchino Y, Yoshikawa K, et al. Discrimination between low-grade oligodendrogliomas and diffuse astrocytoma with the aid of 11C-methionine positron emission tomography. *J Neurosurg*. 2011;114(6):1640-1647. doi:10.3171/2010.11.JNS10553

10. Singhal T, Narayanan TK, Jacobs MP, Bal C, Mantil JC. 11C-methionine PET for grading and prognostication in gliomas: a comparison study with 18F-FDG PET and contrast enhancement on MRI. *J Nucl Med*. 2012;53(11):1709-1715. doi:10.2967/jnumed.111.102533

11. Kato T, Shinoda J, Oka N, et al. Analysis of ^{11} C-methionine Uptake in Low-Grade Gliomas and Correlation with Proliferative Activity. *Am J Neuroradiol*. 2008;29(10):1867-1871. doi:10.3174/ajnr.A1242

12. Lopci E, Riva M, Olivari L, et al. Prognostic value of molecular and imaging biomarkers in patients with supratentorial glioma. *Eur J Nucl Med Mol Imaging*. 2017;44(7). doi:10.1007/s00259-017-3618-3

13. Galldiks N, Stoffels G, Ruge MI, et al. Role of O-(2-18F-fluoroethyl)-L-tyrosine PET as a diagnostic tool for detection of malignant progression in patients with low-grade glioma. *J Nucl Med*. 2013;54(12):2046-2054. doi:10.2967/jnumed.113.123836

14. Pauleit D, Floeth F, Hamacher K, et al. O-(2-[18F]fluoroethyl)-L-tyrosine PET combined with MRI improves the diagnostic assessment of cerebral gliomas. *Brain*. 2005;128(3):678-687. doi:10.1093/brain/awh399

15. Saito T, Maruyama T, Muragaki Y, et al. ^{11} C-Methionine Uptake Correlates with Combined 1p and 19q Loss of Heterozygosity in Oligodendroglial Tumors. *Am J Neuroradiol*. 2013;34(1):85-91. doi:10.3174/ajnr.A3173

16. Kim S, Chung J-K, Im S-H, et al. 11C-methionine PET as a prognostic marker in patients with glioma: comparison with 18F-FDG PET. *Eur J Nucl Med Mol Imaging*.

2005;32(1):52-59. doi:10.1007/s00259-004-1598-6

17. Langen K-J, Galldiks N, Hattingen E, Shah NJ. Advances in neuro-oncology imaging. *Nat Rev Neurol*. 2017;13(5):279-289. doi:10.1038/nrneurol.2017.44

18. Navarria P, Reggiori G, Pessina F, et al. Investigation on the role of integrated PET/MRI for target volume definition and radiotherapy planning in patients with high grade glioma. *Radiother Oncol*. 2014;112(3):425-429. doi:10.1016/j.radonc.2014.09.004

19. Nariai T, Tanaka Y, Wakimoto H, et al. Usefulness of l -[methyl- ^{11} C] methionine—positron emission tomography as a biological monitoring tool in the treatment of glioma. *J Neurosurg*. 2005;103(3):498-507. doi:10.3171/jns.2005.103.3.0498

20. Albert NL, Weller M, Suchorska B, et al. Response Assessment in Neuro-Oncology working group and European Association for Neuro-Oncology recommendations for the clinical use of PET imaging in gliomas. *Neuro Oncol*. 2016;18(9):1199-1208. doi:10.1093/neuonc/now058

21. Weller M, van den Bent M, Tonn JC, et al. European Association for Neuro-Oncology (EANO) guideline on the diagnosis and treatment of adult astrocytic and oligodendroglial gliomas. *Lancet Oncol*. 2017;18(6):e315-e329. doi:10.1016/S1470-2045(17)30194-8

22. Louis DN, Ohgaki H, Wiestler OD, et al. The 2007 WHO classification of tumours of the central nervous system. *Acta Neuropathol*. 2007;114(2):97-109. doi:10.1007/s00401-007-0243-4

23. Bello L, Riva M, Fava E, et al. Tailoring neurophysiological strategies with clinical context enhances resection and safety and expands indications in gliomas involving motor pathways. *Neuro Oncol*. 2014;16(8). doi:10.1093/neuonc/not327

24. Riva M, Fava E, Gallucci M, et al. Monopolar high-frequency language mapping: Can

it help in the surgical management of gliomas? A comparative clinical study. *J Neurosurg*. 2016;124(5). doi:10.3171/2015.4.JNS14333

25. Riva M, Hennersperger C, Milletari F, et al. 3D intra-operative ultrasound and MR image guidance: pursuing an ultrasound-based management of brainshift to enhance neuronavigation. *Int J Comput Assist Radiol Surg*. 2017;12(10):1711-1725. doi:10.1007/s11548-017-1578-5

26. Chang EF, Smith JS, Chang SM, et al. Preoperative prognostic classification system for hemispheric low-grade gliomas in adults. *J Neurosurg*. 2008;109(5):817-824. doi:10.3171/JNS/2008/109/11/0817

27. Smith JS, Chang EF, Lamborn KR, et al. Role of extent of resection in the long-term outcome of low-grade hemispheric gliomas. *J Clin Oncol*. 2008;26(8):1338-1345. doi:10.1200/JCO.2007.13.9337

28. Pallud J, Blonski M, Mandonnet E, et al. Velocity of tumor spontaneous expansion predicts long-term outcomes for diffuse low-grade gliomas. *Neuro Oncol*. 2013;15(5):595-606. doi:10.1093/neuonc/nos331

29. Riva M, Bello L. Low-grade glioma management: A contemporary surgical approach. *Curr Opin Oncol*. 2014;26(6). doi:10.1097/CCO.0000000000000120

30. Eckel-Passow JE, Lachance DH, Molinaro AM, et al. Glioma Groups Based on 1p/19q, *IDH* , and *TERT* Promoter Mutations in Tumors. *N Engl J Med*. 2015;372(26):2499-2508. doi:10.1056/NEJMoa1407279

31. Herholz K, Coope D, Jackson A. Metabolic and molecular imaging in neuro-oncology. *Lancet Neurol*. 2007;6(8):711-724. doi:10.1016/S1474-4422(07)70192-8

32. Galldiks N, Kracht LW, Berthold F, et al. [11C]-L-methionine positron emission tomography in the management of children and young adults with brain tumors. *J Neurooncol*. 2010;96(2):231-239. doi:10.1007/s11060-009-9953-x

33. Johnson BE, Mazor T, Hong C, et al. Mutational analysis reveals the origin and therapy-driven evolution of recurrent glioma. *Science*. 2014;343(6167):189-193. doi:10.1126/science.1239947

34. Inano R, Oishi N, Kunieda T, et al. Visualization of heterogeneity and regional grading of gliomas by multiple features using magnetic resonance-based clustered images. *Sci Rep*. 2016;6(1):30344. doi:10.1038/srep30344

35. Castellano A, Donativi M, Rudà R, et al. Evaluation of low-grade glioma structural changes after chemotherapy using DTI-based histogram analysis and functional diffusion maps. *Eur Radiol*. 2016;26(5). doi:10.1007/s00330-015-3934-6

36. Keunen O, Taxt T, Grüner R, et al. Multimodal imaging of gliomas in the context of evolving cellular and molecular therapies. *Adv Drug Deliv Rev*. 2014;76:98-115. doi:10.1016/j.addr.2014.07.010

37. Bette S, Gempt J, Delbridge C, et al. Prognostic Value of O-(2-[18F]-Fluoroethyl)-L-Tyrosine-Positron Emission Tomography Imaging for Histopathologic Characteristics and Progression-Free Survival in Patients with Low-Grade Glioma. *World Neurosurg*. 2016;89:230-239. doi:10.1016/j.wneu.2016.01.085

38. Verger A, Stoffels G, Bauer EK, et al. Static and dynamic 18F–FET PET for the characterization of gliomas defined by IDH and 1p/19q status. *Eur J Nucl Med Mol Imaging*. 2018;45(3):443-451. doi:10.1007/s00259-017-3846-6

39. Iwadate Y, Shinozaki N, Matsutani T, Uchino Y, Saeki N. Molecular imaging of 1p/19q deletion in oligodendroglial tumours with 11C-methionine positron emission tomography. *J Neurol Neurosurg Psychiatry*. 2016;87(9):1016-1021. doi:10.1136/jnnp-2015-311516

40. Bailey DL, Pichler BJ, Gückel B, et al. Combined PET/MRI: from Status Quo to Status Go. Summary Report of the Fifth International Workshop on PET/MR Imaging;

February 15-19, 2016; Tübingen, Germany. *Mol Imaging Biol*. 2016;18(5):637-650. doi:10.1007/s11307-016-0993-2

41. Lopci E. "The simplest explanation is usually the correct one" - Can Occam's razor be applied for diffuse astrocytoma and paradoxical amino acid metabolism? *Eur J Nucl Med Mol Imaging*. 2017;44(8):1411-1412. doi:10.1007/s00259-017-3708-2

42. Suchorska B, Giese A, Biczok A, et al. Identification of time-to-peak on dynamic 18F-FET-PET as a prognostic marker specifically in IDH1/2 mutant diffuse astrocytoma. *Neuro Oncol*. 2018;20(2):279-288. doi:10.1093/neuonc/nox153

43. Gillies RJ, Kinahan PE, Hricak H. Radiomics: Images Are More than Pictures, They Are Data. *Radiology*. 2016;278(2):563-577. doi:10.1148/radiol.2015151169

44. van den Bent MJ, Baumert B, Erridge SC, et al. Interim results from the CATNON trial (EORTC study 26053-22054) of treatment with concurrent and adjuvant temozolomide for 1p/19q non-co-deleted anaplastic glioma: a phase 3, randomised, open-label intergroup study. *Lancet (London, England)*. 2017;390(10103):1645-1653. doi:10.1016/S0140-6736(17)31442-3

45. Collins FS, Varmus H. A New Initiative on Precision Medicine. *N Engl J Med*. 2015;372(9):793-795. doi:10.1056/NEJMp1500523

FIGURES CAPTION

Figure 1. PET metrics in nonenhancing LGGs.

The pre-operative T1-weighted after contrast injection (**A**), FLAIR (**B**) and 11C-METH-PET (**C**) scans of patient with a grade II, IDH-1 mutated and 1p19q codeleted oligoastrocytoma are reported (A-C). In this case, with no enhancement and a MRI volume of 30.2 cm^3, SUVmax was 2.2, SUVratio was 1.7 and MTB was 15.1.

Although having an overlapping MR phenotype (**D**,**E**,**F**) with no contrast enhancement and a MRI volume of 40.1 cm^3, the PET metrics were higher (SUVmax 2.7, SUVratio 1.8, MTB 29.2) in a patient with a final diagnosis of a grade III oligoastrocytoma, IDH-1/2 wild-type and with no 1p19q codeletion. PET also depicted a structural heterogeneity according to the metabotype, documenting several hypermetabolic foci within the lesion with a homogenous FLAIR MRI appearance.

Figure 2. Relationship between PET metrics and molecular markers.

SUVmax and SUVratio, but not MTB, were statically significant higher in IDH wild type lesion compared to the mutated counterparts (**A**), while exclusively the SUVratio resulted lower in 1p19q codeleted LGGs (**B**).

*$p<0.01$.

n.s.: not statistically significant

Figure 3. PET metrics and molecular integrated diagnosis of LGGs

Despite a trend can be noticed with SUVmax and SUVration, none of the PET metrics herein measured reached a statistically significant threshold, when LGGs of this cohort were partitioned according to the molecular features as recommended by the recently updated WHO brain tumor classification.

Figure 4. Multimodal pre-surgical characterization of LGGs

The results of this study could be used to discuss the role of amminoacid PET in the pre-surgical evaluation of LGGs. Following presentation, the diagnostic radiological work-up includes contrast-enhanced MRI, that provides relevant morphological data, such as lesion site, volume, signs of blood-brain-barrier breakdown as contrast enhancement and speed of growth, when serial scans are volumetrically analyzed.

Amminoacid PET could integrate these data with semiquantitative metrics and a qualitative depiction of the structural heterogeneity. According to the metabolic activity measured from the lesion, this multimodal radiological evaluation could help identifying low- and high-hazard lesions, being the latter those likely with a more aggressive behavior for their histopathology (i.e. grade III) and molecular status (IDH wild-type).

This information could finally support clinical decision making, such as the timing of therapeutic intervention and the guidance of proper tissue sampling to minimize lesion under-staging. In fact, high-hazard lesions should receive prompt treatment, while low-hazard lesion could undergo a close follow-up MRI scan to assess the speed of growth for a more refined tailoring of the treatment options.

Table 1. Clinico-demographic characteristics

Sex	
M/F	61/45
Age	44.01±13.7 years
Treatment naïve subjects	48
Histology and Grade	
Grade II (no.)	45
Oligodendroglioma	26
Astrocytoma	8
Oligoastrocytoma	11
Grade III (no.)	51
Anaplastic Oligodendroglioma	15
Anaplastic Astrocytoma	22
Anaplastic Oligoastrocytoma	14
MRI Lesion volume	29.1 (232.1-1.1) cm3
Lesion side	
R/L	46/50
MRI enhancement	
Present	27
Absent	69

Table 2
Click here to download Table(s): 03_table 2.docx

Table 2. Non-enhancing LGGs on MRI and PET semi-quantitative parameters

	SUVmax	SUVratio	MTB
Grade II	2.4 ±1.2	1.7±0.6	7.1±0.9
Grade III	3.6 ±1.4	2.2±0.6	28.8±1.0
p-value	**0.001**	**0.003**	**<0.001**

Mean values are reported**.**

Table 3. Discrimination of grade with PET, MR and Multimodal Metrics and identification of cut-off values in discriminating lower grade gliomas

	Cut-off	Accuracy	Sensitivity	Specificity
SUVmax	2.7	67.8	55.6	78.4
SUVratio	2.0	71.9	71.1	72.5
MTB	14.9	67.8	64.4	70.6
Gd enhancement	N.A.	69.8	95.6	47.1

Accuracy, sensitivity and specificity values are reported as percentages.

N.A.:not applicable.

Values of MR feature (presence of gadolinium, Gd, enhancement), obtained from this cohort, are reported for comparison.

Table 4. Accuracy, sensitivity and specificity of multimodal characterization, combining PET semiquantitative metrics and MR features (gadolinium enhancement)

	Accuracy	Sensitivity	Specificity
SUVmax	70.8	84.4	58.9
SUVratio	70.8	86.7	56.9
MTB	76.0	86.7	66.7

Values are reported as percentages.

Figure 1_upper row

Click here to download high resolution image

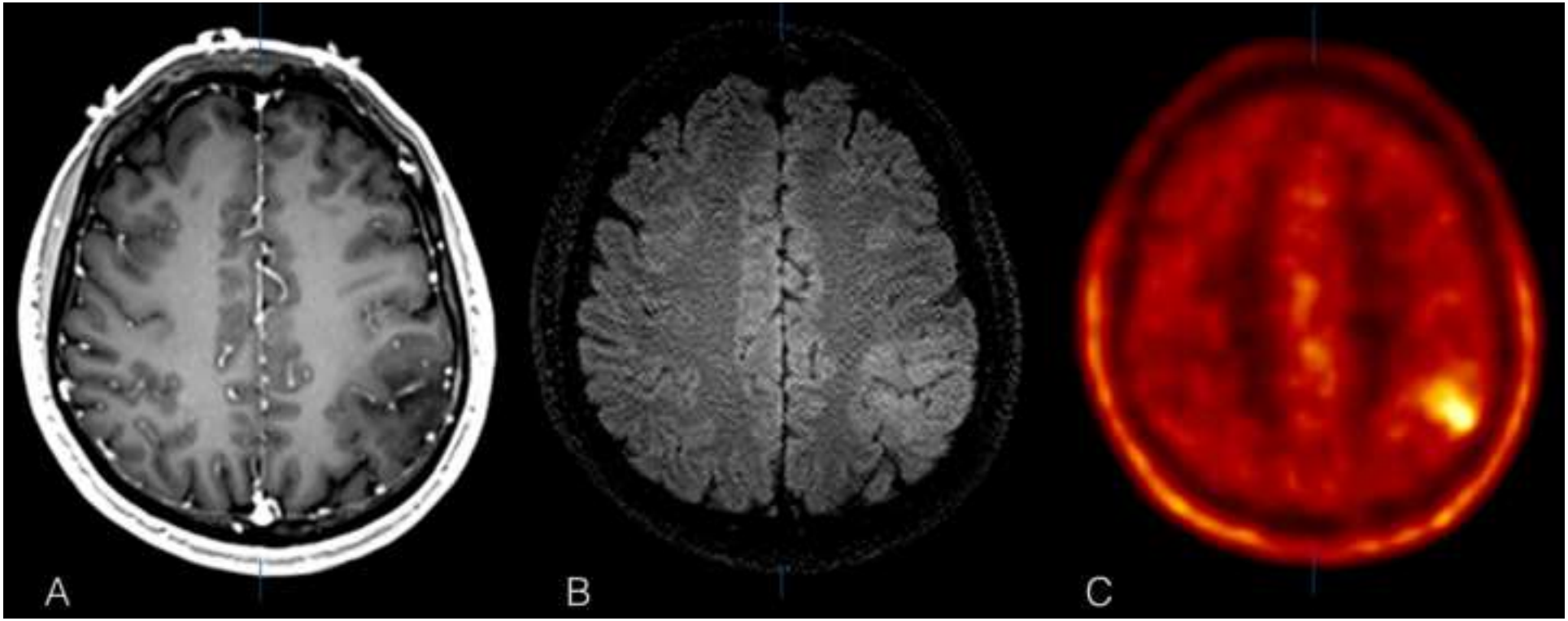

Figure 1_lower row
Click here to download high resolution image

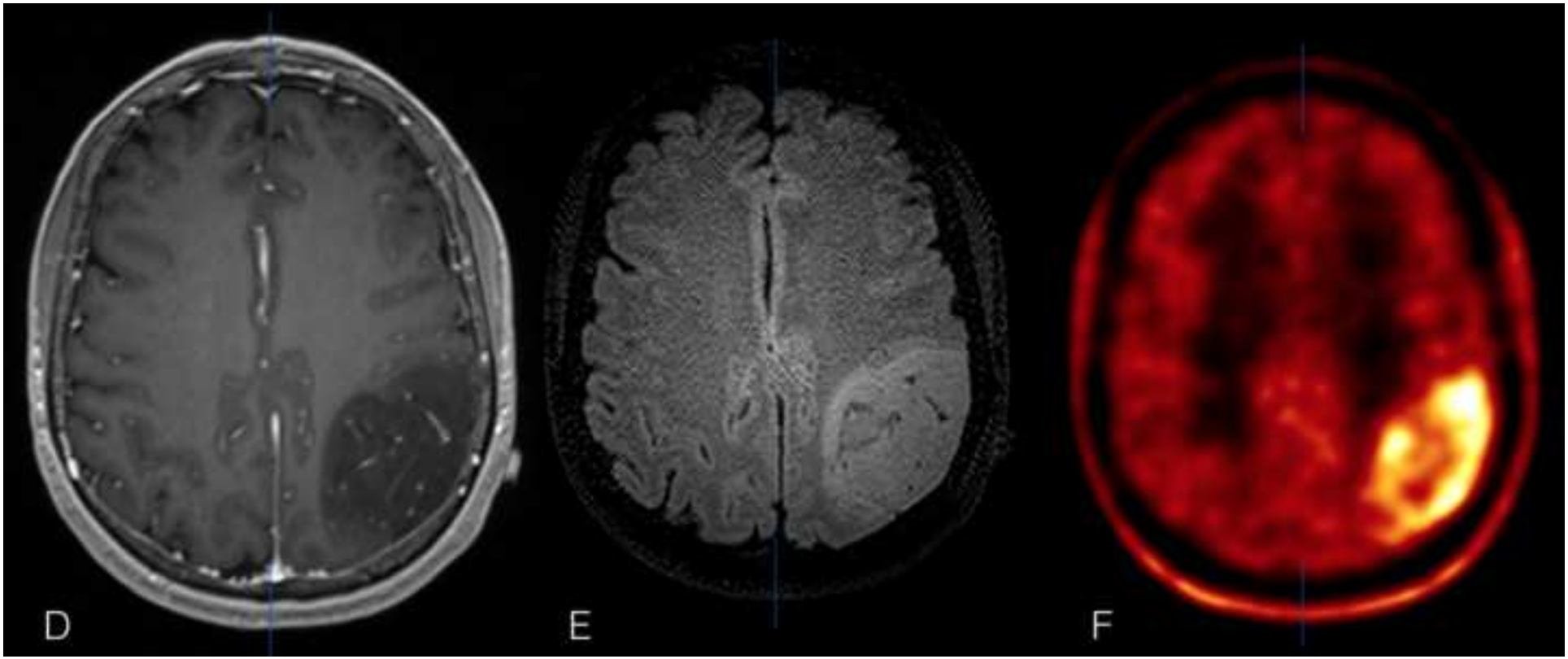

Figure 2A

Click here to download high resolution image

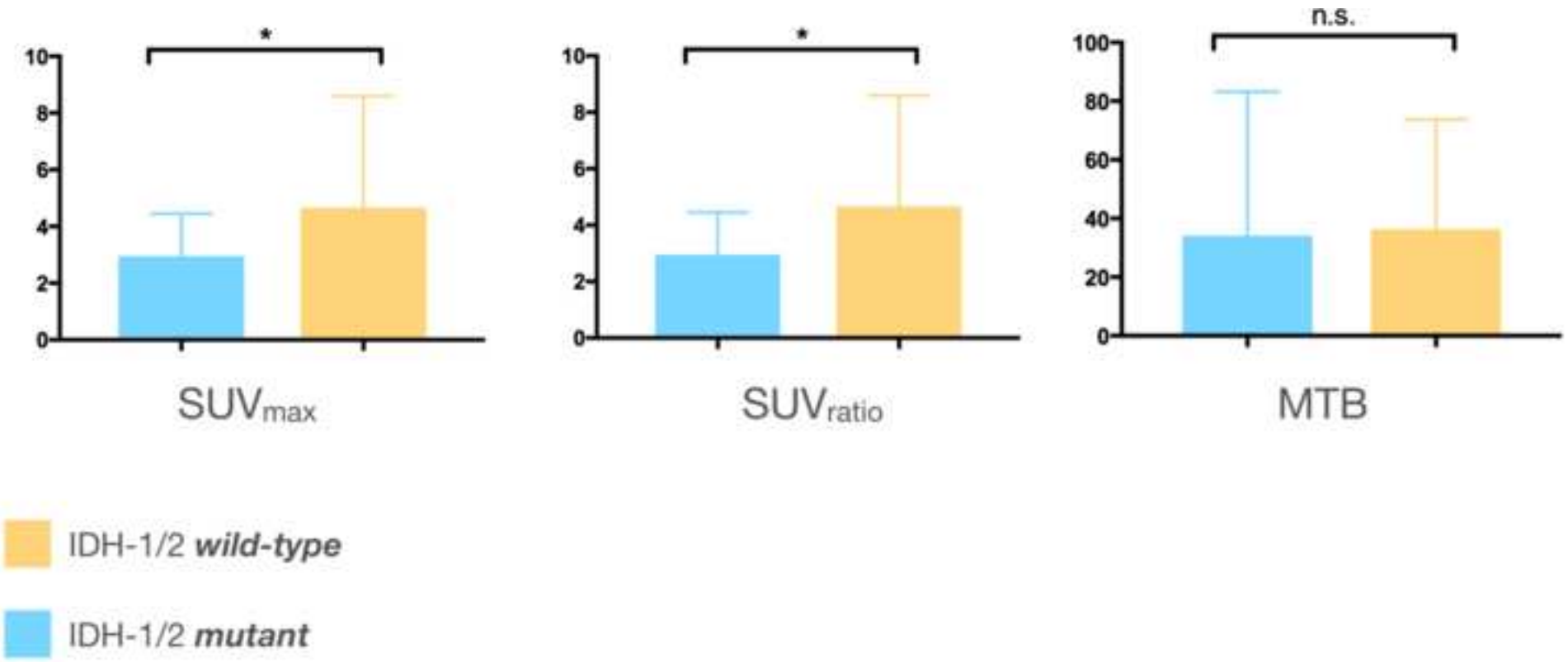

Figure 2B

Click here to download high resolution image

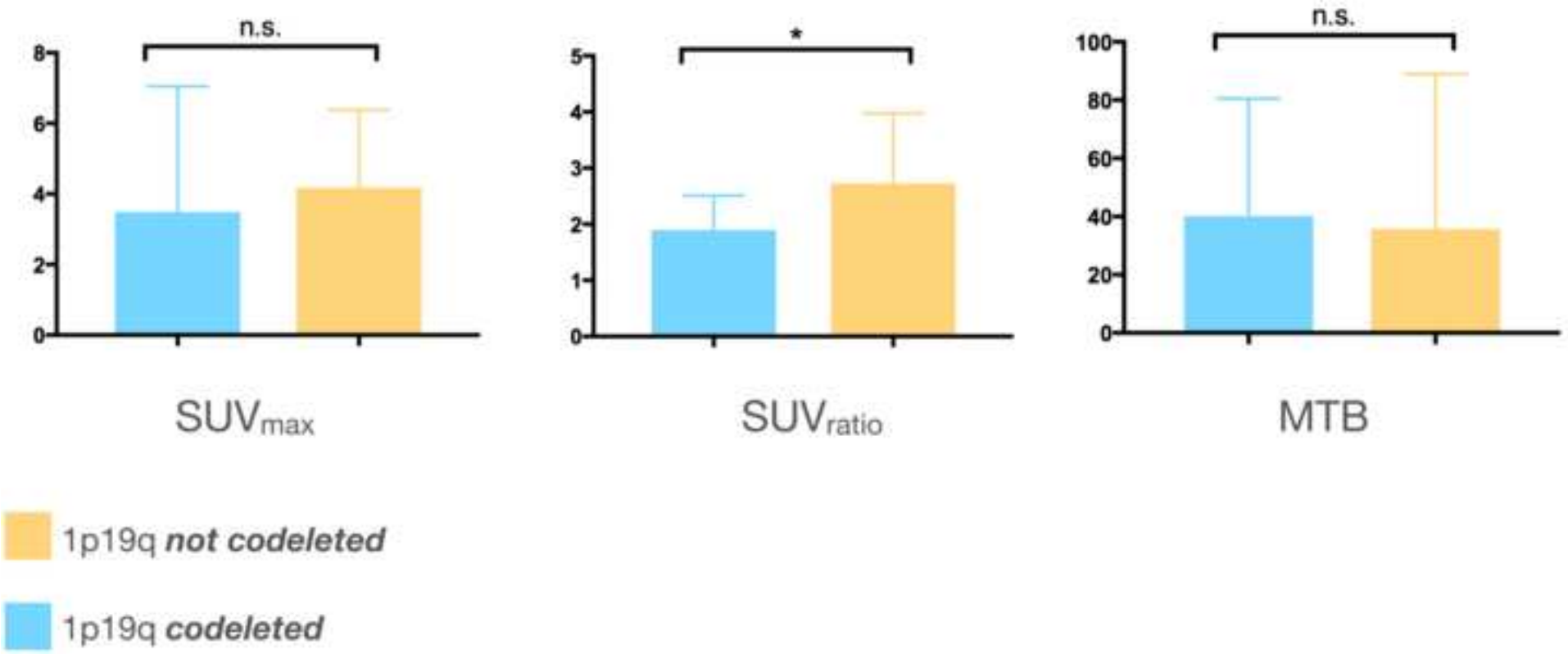

Figure 3

Click here to download high resolution image

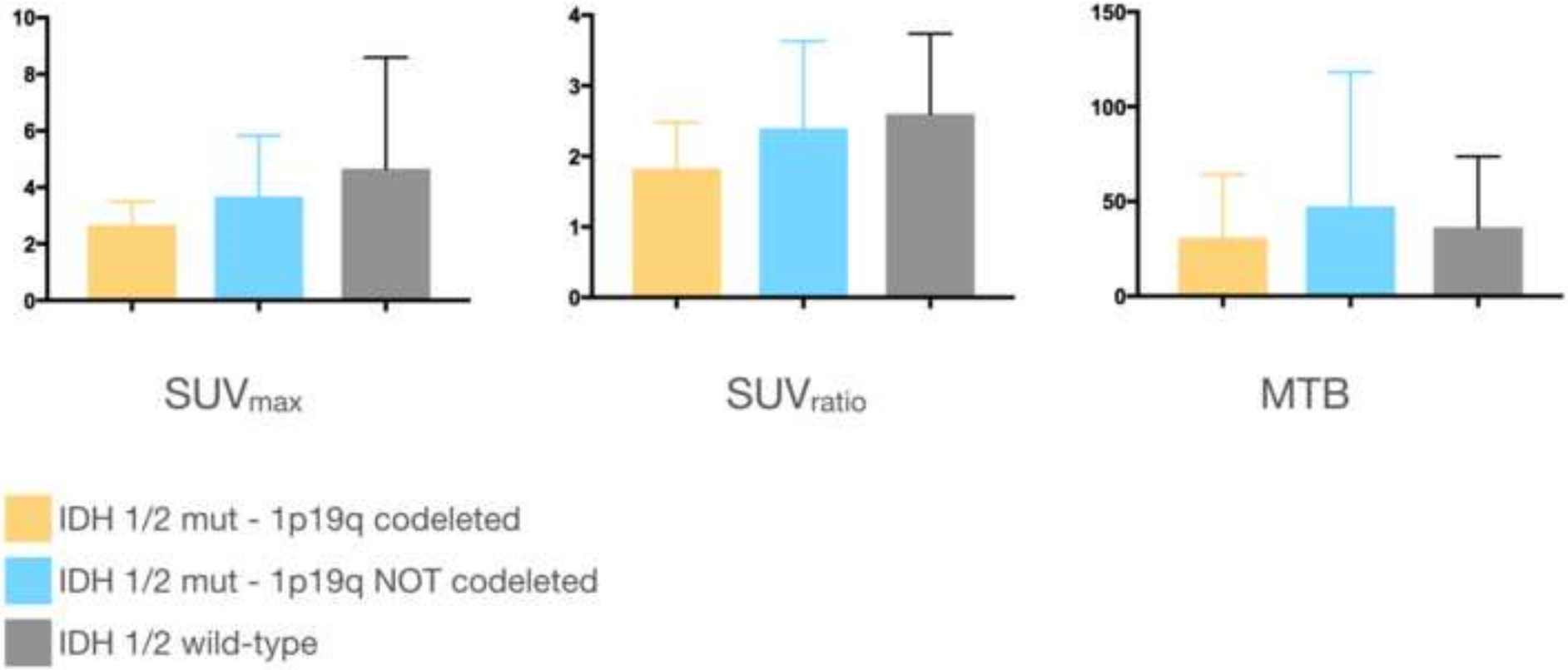

Figure 4

Click here to download high resolution image

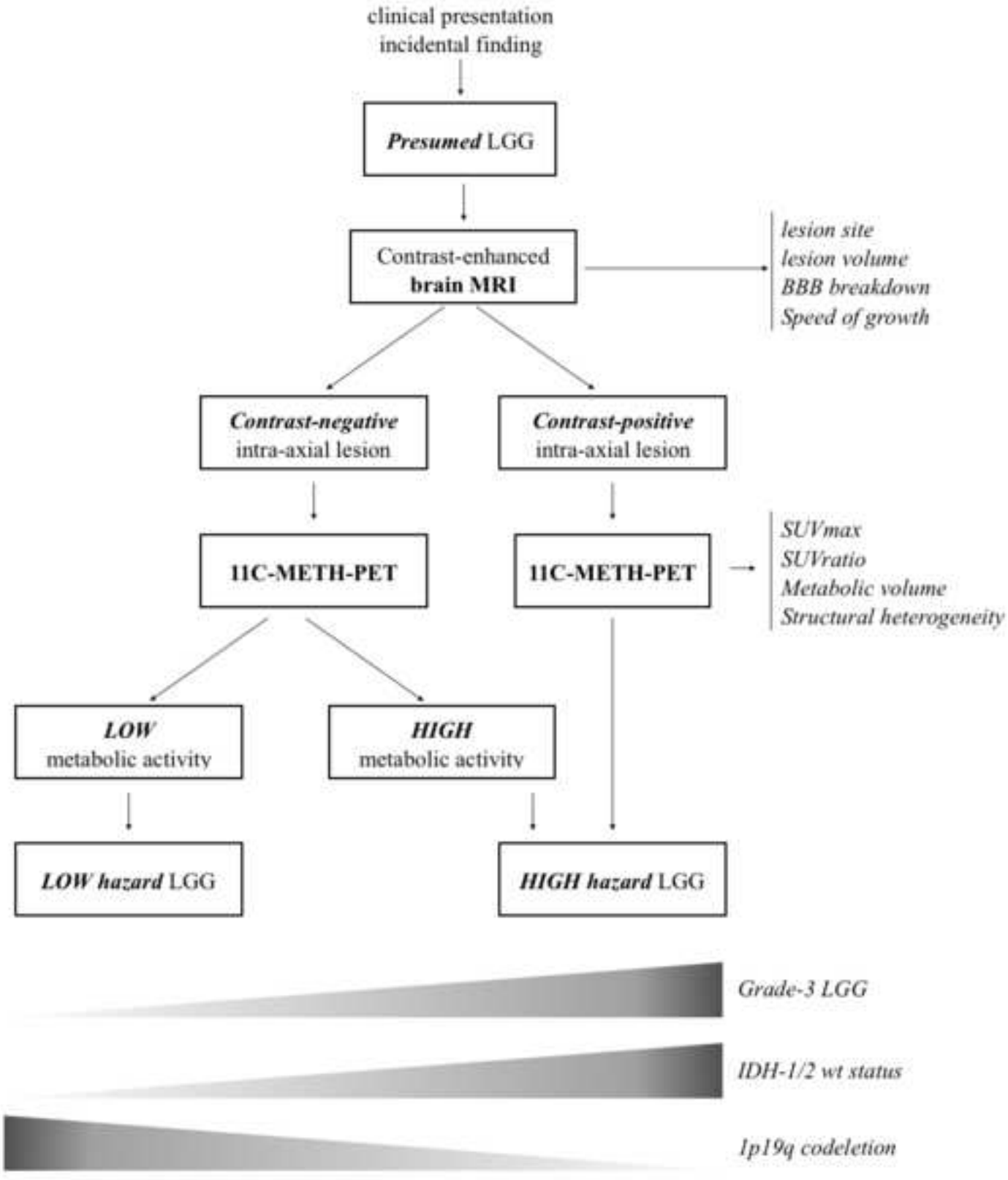

Supplementary Material_Tables

Click here to download Supplementary Material (Video/Media Files): 04_SDC.docx

Supplementary Figure 1A

Click here to download Supplementary Material (Video/Media Files): Figure S1A.tiff

Supplementary Figure 1B

Click here to download Supplementary Material (Video/Media Files): Figure S1B.tiff

Supplementary Figure 1C

Click here to download Supplementary Material (Video/Media Files): Figure S1C.tiff

Supplementary Figure 2

Click here to download Supplementary Material (Video/Media Files): Figure S2.tiff